Published in final edited form as:
Mol Cell. 2011 February 18; 41(4): 458–470. doi:10.1016/j.molcel.2011.01.019.

TBK1 Directly Engages Akt/PKB Survival Signaling to Support Oncogenic Transformation

Yi-Hung Ou[1], **Michael Torres**[1], **Rosalyn Ram**[1], **Etienne Formstecher**[2], **Christina Roland**[3], **Tzuling Cheng**[1], **Rolf Brekken**[3], **Ryan Wurz**[4], **Andrew Tasker**[4], **Tony Polverino**[5], **Seng-Lai Tan**[5,*], and **Michael A. White**[1,*]

[1]Department of Cell Biology, UT Southwestern Medical Center, 5323 Harry Hines Blvd., Dallas, TX 75390, USA

[2]Hybrigenics, Inc. Paris, France

[3]Hamon Center for Therapeutic Oncology Research and Department of Surgery, UT Southwestern Medical Center, 5323 Harry Hines Blvd., Dallas, TX 75390, USA

[4]Amgen, Inc. One Amgen Center Drive, Thousand Oaks, CA 91320, USA

[5]Amgen, Inc. 1201 Amgen Ct. West, Seattle, WA 98119, USA

Abstract

The innate immune signaling kinase, TBK1, couples pathogen surveillance to induction of host defense mechanisms. Pathological activation of TBK1 in cancer can overcome programmed cell death cues, enabling cells to survive oncogenic stress. The mechanistic basis of TBK1 prosurvival signaling, however, has been enigmatic. Here we show that TBK1 directly activates AKT by phosphorylation of the canonical activation loop and hydrophobic motif sites independently of PDK1 and mTORC2. Upon mitogen stimulation, triggering of the innate immune response, re-exposure to glucose, or oncogene activation, TBK1 is recruited to the exocyst, where it activates AKT. In cells lacking TBK1, insulin activates AKT normally, but AKT activation by exocyst-dependent mechanisms is impaired. Discovery and characterization of a 6-aminopyrazolopyrimidine derivative, as a selective low nanomolar TBK1 inhibitor, indicates this regulatory arm can be pharmacologically perturbed independently of canonical PI3K/PDK1 signaling. Thus, AKT is a direct TBK1 substrate that connects TBK1 to prosurvival signaling.

INTRODUCTION

The atypical IκB kinase family member TBK1 (TANK-binding kinase 1) has been defined as a principle hub in cell regulatory networks responsive to inflammatory cytokines and pathogen surveillance receptors (Fitzgerald et al., 2003; Hacker and Karin, 2006; Kawai and Akira, 2007). Together with its homologue IKKε, TBK1 marshals the IRF3 and IRF7 transcription factors to induce type I interferon expression and activation of other components of the immediate early host defense response. As such, TBK1 and IKKε are

*Correspondence to: Michael A. White, Department of Cell Biology, UT Southwestern Medical Center, Dallas, TX 75390-9039, Phone: 214-648-2861, FAX: 214-648-3861, michael.white@utsouthwestern.edu, Seng-Lai Tan, Amgen, Inc., 1201 Amgen Ct. West, Seattle, WA 98119.

required elements of innate immune signaling in most epithelia and stromal cell types (Chau et al., 2008; Hacker and Karin, 2006; Hiscott, 2007; Kawai and Akira, 2007).

In cancer cells, pathological TBK1 activation supports oncogenic transformation by suppressing a programmed cell death response to oncogene activation (Bodemann and White, 2008). TBK1 kinase activity is engaged by Ras through the RalGEF-RalB-Sec5 effector pathway, is elevated in transformed cells, and is required for their survival in culture (Chien et al., 2006; Korherr et al., 2006). Systematic RNAi screens of diverse tumor-derived cell lines confirmed that a codependent relationship between oncogenic Ras and the RalB/Sec5/TBK1 pathway is conserved in a variety of disease settings (Barbie et al., 2009).

While IRF3 is a direct TBK1 substrate that clearly accounts for much of the role of TBK1 in support of innate immune signaling (Fitzgerald et al., 2003; Sharma et al., 2003), TBK1 substrates that mediate cancer cell survival are ill defined. Studies employing IRF3$^{-/-}$ MEFs or RNAi-mediated IRF3 depletion from cancer cell lines indicated this canonical TBK1 substrate is not an obligate component of TBK1-driven cell survival signaling (Barbie et al., 2009; Chien et al., 2006), but may be important for pro-angiogenic signaling (Korherr et al., 2006). Using TBK1$^{-/-}$ cells to parse TBK1-dependent Ras-induced regulatory events, we found TBK1 is required for oncogenic Ras activation of AKT and concomitant mTOR activation and GSK3β suppression. Insulin-induced AKT activation is intact in TBK1$^{-/-}$ MEFs, however TLR4, TLR3, EGFR and glucose-induced AKT activation is impaired. In human epithelial cells, these TBK1-dependent signals recruit endogenous TBK1 to the exocyst where it activates AKT. Furthermore, TBK1 depletion impairs both mitogen and oncogene activation of AKT in human cells. We find that TBK1 directly interacts with AKT and is sufficient to drive both activation loop, T308, and hydrophobic motif, S473, phosphorylation in cells and within an *in vitro* biochemical reconstitution system. Consistent with these observations, TBK1 activation of AKT in cells can occur in the absence of the canonical AKT-T308 and AKT-S473 kinases, PDK1 and mTORC2. Loss of TBK1 is toxic to most, but not all oncogenic Ras expressing tumor lines *in vitro* and *in vivo*, and this toxicity can be rescued by expression of mutationally activated AKT. A chemical inhibitor of TBK1 kinase activity, with potency in the nanomolar range, was isolated from a 250,000 compound screen. This 6-aminopyrazolopyrimidine derivative is selectively toxic to TBK1-dependent cancer cell lines. Furthermore, the compound can inhibit AKT activation in these cells without affecting the canonical AKT activators PDK1 or mTOR. Thus AKT likely represents a bona fide TBK1 substrate protein that mediates TBK1-dependent signaling in normal and tumorigenic contexts. The phenotypic concordance of TBK1 homozygous deletion, RNAi-mediated TBK1 depletion and pharmacological inhibition of TBK1 kinase activity reveals TBK1 as a targetable link supporting context-selective mobilization of the AKT regulatory network.

RESULTS

Previous observations that TBK1$^{-/-}$ MEFs fail to support oncogenic Ras-induced transformation, at least in part due to survival defects (Chien et al., 2006), prompted us to examine survival pathway activation in this setting. As expected, lentiviral-mediated transient expression of K-RasG12V in wild-type mouse embryo fibroblasts resulted in excess AKT activation as indicated by accumulation of activation site phosphorylation (Downward, 2003; Manning and Cantley, 2007; Mitin et al., 2005). In contrast, despite equivalent K-RasG12V expression, TBK1$^{-/-}$ MEFs did not support AKT activation by oncogenic Ras (Figure 1A). Selection of stable populations of wild-type and TBK1$^{-/-}$ MEFs, with similar amounts of K-RasG12V expression, showed marked differences in the formation of growth transformed foci, accumulation of active AKT, and concomitant engagement of the mTOR pathway (Figure 1B). Transient siRNA-mediated TBK1 depletion

in human osteosarcoma cells and telomerase-immortalized airway epithelial cells with multiple independent siRNAs resulted in reduced accumulation of active AKT as compared to controls (Figure 1C). Collectively, these observations suggest TBK1 supports AKT pathway activation in multiple regulatory contexts.

We have previously defined the heterooctameric Sec6/8 a.k.a. exocyst complex as a hub for Ras activation of TBK1 via the RalB effector pathway (Chien et al., 2006; Chien and White, 2003; Moskalenko et al., 2002). A protein/protein interaction map, generated by saturating genome-wide yeast two-hybrid screens of each human exocyst subunit against a human placenta library, identified AKT1 and AKT2 interactions with two distinct exocyst subunits-Exo70 and Sec3 (Figure 1D). The association of AKT with the exocyst was validated by expression co-IP (Figure 1E) as well as recovery of native exocyst components from endogenous AKT immunoprecipitates (see Figure 3D). The functional relevance of this association is suggested by impaired accumulation of active AKT upon Sec3 depletion from U2OS cells (Figure 1C). Immunoprecipitates of native exocyst complexes from multiple cell types selectively coprecipitated endogenous TBK1 versus the closely related family member, IKKε, further implicating TBK1 and the exocyst in AKT activation (Figure 1F).

To assess the context-selective contribution of TBK1 to AKT activation, we evaluated the responsiveness of TBK1$^{-/-}$ cells to a variety of germane AKT pathway agonists (Figure 2). We found that AKT was equivalently responsive to insulin in both wild-type and TBK1$^{-/-}$ MEFs, indicating that insulin-induced AKT activation is TBK1-independent (Figure 2A). In contrast, AKT-responsiveness to EGF or glucose was impaired in the absence of TBK1 (Figure 2B,D). In addition, AKT-responsiveness to innate immune pathway activation by either Sendai virus infection or LPS exposure was severely blunted in the absence of TBK1 as compared to wild-type MEFs (Figure 2F). Complementation of TBK1$^{-/-}$ MEFs using human wild-type TBK1 rescued AKT activation by EGF and glucose (Figure 2C,E). We did not observe activation of IFNβ expression, a canonical TBK1 effector pathway, in response to EGF or glucose reexposure in these cells (Figure 2G). However, TBK1$^{-/-}$ MEFs were refractory to EGF-induced proliferation (Figure 2H) and sensitized to apoptosis upon serum or glucose withdrawal (Figure 2I). Together, these observations reveal a stimulus-selective contribution of TBK1 to AKT pathway activation.

Examination of full-length and truncated proteins indicated that TBK1 and AKT can be reciprocally isolated in either TBK1 or AKT immunoprecipitates (Figure 3A) and that the association in cells is likely mediated through their respective kinase domains (Figure 3B,C). To examine native TBK1/AKT complex assembly, we tested the capacity of endogenous AKT to coimmunoprecipitate endogenous TBK1 in response to glucose exposure or innate immune pathway activation- two settings requiring TBK1 for AKT activation as indicated by observations in TBK1$^{-/-}$ MEFs (Figure 2). In glucose starved cells, the exocyst but not TBK1 coimmunoprecipitated with AKT. However, glucose stimulation recruited TBK1 to AKT complexes in all 4 human cell lines tested (Figure 3D). Sorbitol exposure was used as an osmolarity control (Figure 3D, middle top panel). These observations indicate that a population of AKT is constitutively associated with the exocyst, while TBK1 is recruited into the complex in a stimulus-dependent manner. Similarly, Sendai virus infection or LPS exposure drove assembly of native TBK1/AKT complexes (Figure 3E).

Both wild-type and kinase-dead TBK1 associated with AKT, however, only wild-type TBK1 immunoprecipitates contained active AKT, as indicated by serine 473 phosphorylation and *in vitro* kinase activity using a GSK3α/β fusion peptide as substrate (Figure 4A). Remarkably, TBK1 expression was sufficient to drive AKT activation in the face of pharmacological inactivation of the PI3K family (Figure 4B). Moreover, TBK1

induced AKT activation loop (T308) and hydrophobic motif (S473) phosphorylation in cells in the absence of PDK1 (Figure 4C,D) or the mTORC2 subunits Sin1 (Figure 4E) or Rictor (Figure 4F). These observations indicate that TBK1 is sufficient to induce AKT activation independently of the canonical PDK1/mTORC2 collaboration (Alessi et al., 1997; Engelman, 2009; Guertin et al., 2006; Jacinto et al., 2006; Manning and Cantley, 2007; Sarbassov et al., 2005; Shiota et al., 2006).

In the presence of ATP and Mg^{++}, purified recombinant TBK1 was sufficient to drive phosphorylation of both T308 and S473 on otherwise inactive recombinant AKT1 *in vitro* (Figure 4G). Moreover, this correlated with a 100-fold increase in AKT1 specific activity as detected using a GSK3α/β–derived peptide substrate (Figure 4G), and with significant accumulation of phosphorylation of AKT autosubstrate sites (Figure 4H) (Li et al., 2006). Endogenous TBK1 immunoprecipitated from MEFs also directly phosphorylated recombinant AKT (Figure 4I). Consistent with a role for TBK1 in EGF-induced AKT activation in MEFs (Figure 2B) TBK1 kinase activity was enhanced by EGF stimulation (Figure 4I). Similar observations using kinase-dead and wild-type proteins immunopurified from HEK293T cells indicated that TBK1-induced phosphorylation of AKT-T308 and AKT-S473 was dependent upon an intact TBK1 kinase domain, and independent of AKT kinase activity (Figure 4J). As expected, TBK1 induction of AKT autosubstrate site phosphorylation only occurred with catalytically intact AKT (Figure 4J). Thus, TBK1 appears to be sufficient to directly activate AKT. The disease significance of this non-canonical regulatory arm is suggested by the observation that, in the absence of PDK1, oncogenic Ras signaling to AKT is only partially blunted and the responsiveness of AKT effectors is unaffected (Figure 4K).

To examine the consequence of TBK1 on tumorigenicity, we first depleted TBK1 using lentiviral transduction of shRNAs in Mia-Paca2 cells, a pancreas cancer cell line with the K-RasG12C mutation (Forbes et al., 2009). Two of three hairpins resulted in detectable TBK1 depletion by 2 days post transduction with concomitant reduction in AKT activation (Figure 5A). By 6 days post transduction, the viability of TBK1 depleted cells was severely compromised (Figure 5B), but could be rescued by expression of an artificially activated myristoylated AKT fusion protein (Figure 5C). To examine if the cell death observed in cultured cells was recapitulated in an orthotopic setting, Mia-Paca-2 cells were surgically implanted beneath the capsule of the tail of the pancreas of immune-compromised mice two days post transduction with shRNA expressing lentiviral constructs. Two independent TBK1 shRNAs impaired primary tumor initiation (Figure 5D) and progression (Figure 5E) as compared to controls. Equivalent experiments were also performed in MDA-MB-231 cells, a triple negative breast cancer derived cell line with activating mutations in both K-Ras and B-Raf (Forbes et al., 2009). MDA-MB-231 cells, transduced with shRNA-expressing lentivirus, were implanted into the mammary fat pad of immune compromised mice and tumor growth was followed (Figure 5F). By 45 days post-implantation, control samples had progressed substantially (Figure 5G) and metastasized to other organs (Figure 5H). In contrast, TBK1-depleted samples progressed very poorly and failed to metastasize (Figure 5F,G,H). These observations indicate that TBK1 is required to support AKT activation in cancer cells, and is required for primary tumor initiation and progression, at least in the context of two different orthotopic xenograft models.

To discriminate the consequence of TBK1 depletion from inhibition of TBK1 kinase activity, we wished to employ small molecule TBK1 inhibitors for pharmacological interrogation of the TBK1/AKT regulatory relationship in normal and cancer cells. The currently available compound, BX795 (Bamborough et al., 2006; Clark et al., 2009), has significant activity against both TBK1 and PDK1, which limits its application to these studies (Bain et al., 2007). Therefore, we isolated additional chemical TBK1 inhibitors from

a biochemical screen of ~250,000 small molecules. A 6-aminopyrazolopyrimidine derivative (Compound II, Figure 6A) was identified as a lead compound with an IC_{50} of 13 nM against TBK1 and 59 nM against the TBK1 homolog IKKε, but with 100- to 1000-fold less activity against other tested protein kinases including PDK1, PI3K family members and mTOR (Figure 6B). Consistent with inhibition of TBK1-dependent signaling, compound II inhibited LPS-induced expression of IFNβ(IC_{50} =62nM), and the IFNβ target genes IP10 (IC_{50} =78nM) and Mx1 (IC_{50} =20nM) (Figure 6C). Consistent with selective activity on canonical TBK1 pathway activation (Sato et al., 2003; Yamamoto et al., 2003), Compound II effectively blockedTLR3-dependent IRF3 nuclear translocation in cells with an IC_{50} under 100 nM, but did not impair TNFR1-dependent p65 NFκB nuclear translocation with doses as high as 20 μM (Figure 6D). This later response has been defined as TBK1-independent (Chien et al., 2006; Perry et al., 2004; Sato et al., 2003). Concordant with our observations in $TBK1^{-/-}$ MEFs, a 30-minute pretreatment of wild-type MEFs with Compound II impaired AKT activation by glucose (Figure 6E). Similarly, a 30-minute incubation of the TBK1-sensitive cell line HCC44 with doses of Compound II as low as 500 nM was sufficient to blunt baseline AKT activity (Figure 6F). Notably, Compound II had no activity against the canonical AKT kinases PDK1 and mTOR *in vitro* (Figure 6B), indicating the defective AKT response is likely a consequence of impaired TBK1 activity. Concordant with mTORC2-independent activation of AKT by TBK1, the AKT response to host defense signaling in $Sin1^{-/-}$ and $Rictor^{-/-}$ cells was blocked by Compound II (Figure 6G). Concordant with the consequence of siRNA and shRNA-mediated TBK1 depletion, a 24-hour exposure to Compound II inhibited AKT pathway activation and survival in multiple cancer cell lines at doses close to those affecting IRF-3 nuclear localization (Figure 6H). Importantly, the extent of AKT inhibition was equivalent or better than that observed with 40 μM of the PI3K inhibitor LY294002 (Figure 6H).

We next examined if cancer cell lines selectively sensitive to shRNA-mediated TBK1 depletion were also selectively sensitive to Compound II. First, to assess the incidence of TBK1-sensitivity across diverse oncogenotypes within a discrete disease setting, we employed a panel non-small cell lung cancer (NSCLC) derived cells lines for which the oncogenic Ras status had been defined. We collected 15 lines, 10 of which express oncogenic K-Ras, and examined the consequence of TBK1 depletion on cell viability using two independent TBK1 shRNAs. We found that TBK1 depletion was toxic to approximately 50% of this cohort (Figure 7A). Of note, H1993 (TBK1-sensitive) and H2073 (TBK1-resistant) are derived from a lymph node metastasis and the primary tumor, respectively, from the same patient. Although many lines with oncogenic Ras mutations were in the TBK1-dependent class (6 of 10), the presence of this oncogene is not solely sufficient to specify TBK1-sensitivity. A recent study examining the relative addiction of NSCLC cell lines to oncogenic Ras expression indicated that lines with epithelial characteristics, including elevated E-cadherin expression, were selectively dependent on the continued expression of oncogenic Ras (Singh et al., 2009). However, this relationship also failed to specify TBK1-sensitivity (Figure 7A, lower panels), suggesting additional key biological determinants driving TBK1 addiction remain to be discovered. A549 (TBK1-dependent) and H441 (TBK1-independent) were exposed to Compound II for 96 hours across a nanomolar to micromolar dose range, with cell viability as the endpoint assay. Importantly A549 cells (IC_{50} ~ 0.4 micromolar) were acutely responsive to compound II concentrations at least 10 fold lower than those required for significant toxicity in H441 cells (IC_{50} ~ 4.2 micromolar) (Figure 7B). In addition, TBK1-dependent lines were selectively sensitive to induction of apoptosis upon a 24-hour exposure to 2 micromolar Compound II as compared to TBK1-independent lines (Figure 7C). Compound II exposure strongly suppressed accumulation of active AKT in all TBK1-sensitive NSCLC lines tested (H358, H1993, and HCC44). In contrast the TBK1-independent cell lines H2073 and H441 maintained chronic AKT activation in the presence of Compound II (Figure 7D). Calu1, which displays intermediate

sensitivity to TBK1 depletion (Figure 7A), also displayed intermediate sensitivity to Compound II-dependent inhibition of AKT activation (Figure 7D). These concordant observations between RNAi-mediated TBK1 depletion and small molecule mediated inhibition of TBK1 activity indicate that TBK1 represents an important direct regulatory input to AKT survival signaling.

DISCUSSION

Beyond its canonical occupation as a core component of innate immune and inflammatory cytokine signaling, TBK1 has attracted attention as a potential therapeutic target in cancer given its selective support of cancer cell viability (Barbie et al., 2009; Chien et al., 2006). Here, we have identified the survival signaling kinase AKT/PKB as a direct TBK1 effector. Upon genetic ablation, RNAi-mediated depletion, or pharmacological inactivation of TBK1, AKT activity is diminished and cancer cell viability is impaired. The mechanistic basis of TBK1 support of AKT activation is direct stimulation of AKT catalytic activity as a consequence of TBK1-induced phosphorylation of both the T308 activation loop residue and the S473 hydrophobic domain residue. TBK1 expression is required to support pathological oncogene-dependent AKT signaling, and is required to fully engage AKT in response to EGF, glucose, and host defense signaling. Insulin responsiveness, on the other hand, is TBK1-independent.

The PDK1 kinase and mTORC2 complex have been defined as key proximal determinants of AKT activation. mTORC2 directly phosphorylates AKT-S473, which in turn promotes direct phosphorylation of T308 by PDK1 in the presence of appropriate collateral accumulation of the PI3K product phosphatidylinositol-3,4,5-trisphosphate (PIP_3) (Alessi et al., 1997; Engelman, 2009; Manning and Cantley, 2007; Sarbassov et al., 2005). This collaborative action is required for AKT activation by insulin (Hresko and Mueckler, 2005), though the mechanism of mTORC2 activation in this context is currently unknown (Manning and Cantley, 2007). Our observations suggest that the contribution of TBK1 to AKT activation is non-redundant to the PDK1/mTORC2 pathway. For example, the PDK1/mTORC2 pathway is apparently intact in $TBK1^{-/-}$ MEFs given the wild-type responsiveness of AKT to insulin in these cells. However, the defective AKT responsiveness to EGF, glucose, or innate immune signaling indicates that PDK1/mTORC2 are not sufficient to engage AKT downstream of all germane regulatory inputs. Most importantly, TBK1 retains the capacity to activate AKT in cells where PDK1 or the mTORC2 subunits Sin1 or Rictor have been homozygously deleted.

We find that a subpopulation of AKT in cells is associated with the Sec6/8 a.k.a. exocyst complex. This heterooctameric protein complex was originally identified through its role in the regulated targeting and tethering of selected secretory vesicles to specialized dynamic plasma membrane domains (Grindstaff et al., 1998; Guo et al., 2000). Subsequently, it was discovered that the exocyst plays a direct role in host defense signaling by marshaling TBK1 and STING (stimulator of interferon genes) in response to cellular detection of viral replication intermediates (Bodemann and White, 2008; Chien et al., 2006; Ishikawa and Barber, 2008; Ishikawa et al., 2009). The recruitment of TBK1 to the exocyst in response to AKT pathway agonists that are TBK1 dependent, together with the observation that exocyst integrity supports AKT activation, suggests that this protein complex may represent an architecturally discrete signaling platform. Distinct regulatory inputs to AKT, which can be separately or simultaneously operative, could support compartmentalization of AKT activity within a cell, perhaps as a mechanism to specify the cadre of client substrates engaged by AKT in response to diverse agonists (Bozulic and Hemmings, 2009; Jacinto et al., 2006).

Chemical inhibitors of TBK1 will be valuable in further clarifying the role of TBK1 in AKT survival signaling, and defining the therapeutic value of this kinase target. As a tool compound, Compound II was found to be effective in the low nanomolar range in vitro, cell permeable, and a potent and selective TBK1 inhibitor in cells. Importantly, Compound II exposure impaired accumulation of active AKT, and displayed selective toxicity in TBK1-dependent cancer cell lines. The concordant observations with Compound II exposure and TBK1 depletion strongly suggest that the phenotypes reported here are most likely a consequence of TBK1 catalytic activity as opposed to activity-independent consequences of TBK1 depletion. This indicates that TBK1 support of pathological AKT activation can likely be pharmacologically targeted in disease. In conclusion, our observations define AKT as a direct TBK1 effector and reveal a non-canonical context-selective regulatory mechanism for mobilization of AKT signaling.

EXPERIMENTAL PROCEDURES

Materials

Plasmids, reagents, antibodies, cell cultures and transfections are described in detail in supplemental methods.

Immunoprecipitation and affinity purification

Whole cell extracts were prepared in non-denaturing IP buffer (20 mM Tris HCl [pH 7.5], 10 mM MgCl2, 2 mM EGTA, 10% Glycerol, 137 mM NaCl, 1% Triton X-100 (vol/vol), 0.5% Na Deoxycholate, 1 mM DTT, phosphatase and protease inhibitors [Roche]) were incubated with anti-AKT1 mouse monoclonal antibody (Cell Signaling) and 30 μl Protein A/G beads (Santa Cruz) overnight at 4°C. Immunoprecipitates were washed three times in (20 mM Tris HCl [pH 7.5], 10 mM $MgCl_2$, 2 mM EGTA, 10% Glycerol, 137 mM NaCl, 1% Triton X-100 (vol/vol), 0.5% Na Deoxycholate, 1 mM DTT, and 1 mM PMSF) then boiled in standard SDS sample buffer.

In Vitro protein kinase activity assays

20 ng of His-tagged TBK1 and 100 ng of His-tagged AKT were mixed as indicated in kinase buffer (25 mM Tris HCl [pH 7.5], 10 mM $MgCl_2$, 5 mM β-Glycerophosphate, 2 mM DTT, and 0.1 mM $Na3VO_4$) containing 200 μM ATP at 3°C. After 30 min., 1 μg of GST-GSK3α/β AKT substrate peptide (CGPKGPGRRRTSSFAEG) and 200 μM ATP were added and incubated for additional 30 min at 30°C. Phosphorylation of the AKT substrate sites on the GSK3α/β peptide was detected using the phospho-GSK-3α/β (Ser21/9) antibody (Cell Signaling).

Chemical compound screen

A library of 256,953 kinase inhibitor-biased compounds were screened against full-length TBK1 (Invitrogen) using an HTRF assay from the CisBio KinEase system. Compounds were screened at single dose of 25 μM in the presence of 6 nM TBK1, 1 μM STK3, and 10 μM ATP (2xKm) using the HTRF KinEASE S3 kit. 917 compounds which inhibited >40% of TBK1 activity were selected for single-point reconfirmation. Dose-response studies were performed on 818 confirmed hits, and compounds with $IC_{50} < 1$ μM were selected for follow-up studies. Compound II was found to be a potent inhibitor of TBK1 and IKKε in both biochemical and cell-based assays. In-house kinase cross-screening revealed a reasonable selectivity profile in that Compound II does not inhibit IKK α/β kinases and known kinase mediators of the PI3K-AKT-mTOR pathway.

Yeast two-hybrid screens

The coding sequences for amino acids 1–222 of human AKT1 (GenBank gi:6224101) and amino acids 111 – 222 of human AKT2 (GenBank gi: 6715585) were cloned into pB6 as a C-terminal fusion to Gal4 DNA Binding Domain. The constructs were used as baits to screen at saturation a highly complex, random-primed human placenta cDNA library as previously described (Fromont-Racine et al., 1997).

Orthotopic xenograft tumor models

For the orthotopic breast cancer model, 5×10^6 naïve or infected MDA-MB-231 cells were injected into the mammary fat pad (MFP) of SCID mice using previously described techniques (Roland et al., 2009). For the orthotopic pancreatic cancer model, 1×10^6 naïve or infected Mia-Paca-2 cells in 50 μl PBS were injected into the tail of the pancreas using previously described techniques (Dineen et al., 2008).

Supplementary Material

Refer to Web version on PubMed Central for supplementary material.

Acknowledgments

We are grateful to Zhijian James Chen, Xuetao Cao, Philip N. Tsichlis, Charles Yeaman, William Hahn, Keqiang Ye, and Shu-Chan Hsu, Bing Su, Dos Sarbassov, Mark Magnuson, David Sabatini and Bert Vogelstein for many of the reagents used in these studies. We thank Melanie H. Cobb, Philip N. Tsichlis, Lawrence Lum, and members of our laboratory for invaluable advice and discussion. This work was supported by the National Institutes of Health (CA71443 and CA129451) and the Robert Welch Foundation (I-1414).

REFERENCES

Alessi DR, James SR, Downes CP, Holmes AB, Gaffney PR, Reese CB, Cohen P. Characterization of a 3-phosphoinositide-dependent protein kinase which phosphorylates and activates protein kinase Balpha. Curr Biol. 1997; 7:261–269. [PubMed: 9094314]

Bain J, Plater L, Elliott M, Shpiro N, Hastie CJ, McLauchlan H, Klevernic I, Arthur JS, Alessi DR, Cohen P. The selectivity of protein kinase inhibitors: a further update. Biochem J. 2007; 408:297–315. [PubMed: 17850214]

Bamborough P, Christopher JA, Cutler GJ, Dickson MC, Mellor GW, Morey JV, Patel CB, Shewchuk LM. 5-(1H-Benzimidazol-1-yl)-3-alkoxy-2-thiophenecarbonitriles as potent, selective, inhibitors of IKK-epsilon kinase. Bioorg Med Chem Lett. 2006; 16:6236–6240. [PubMed: 16997559]

Barbie DA, Tamayo P, Boehm JS, Kim SY, Moody SE, Dunn IF, Schinzel AC, Sandy P, Meylan E, Scholl C, et al. Systematic RNA interference reveals that oncogenic KRAS-driven cancers require TBK1. Nature. 2009; 462:108–112. [PubMed: 19847166]

Bellacosa A, Chan TO, Ahmed NN, Datta K, Malstrom S, Stokoe D, McCormick F, Feng J, Tsichlis P. Akt activation by growth factors is a multiple-step process: the role of the PH domain. Oncogene. 1998; 17:313–325. [PubMed: 9690513]

Bodemann BO, White MA. Ral GTPases and cancer: linchpin support of the tumorigenic platform. Nat Rev Cancer. 2008; 8:133–140. [PubMed: 18219307]

Bozulic L, Hemmings BA. PIKKing on PKB: regulation of PKB activity by phosphorylation. Curr Opin Cell Biol. 2009; 21:256–261. [PubMed: 19303758]

Chau TL, Gioia R, Gatot JS, Patrascu F, Carpentier I, Chapelle JP, O'Neill L, Beyaert R, Piette J, Chariot A. Are the IKKs and IKK-related kinases TBK1 and IKK-epsilon similarly activated? Trends Biochem Sci. 2008; 33:171–180. [PubMed: 18353649]

Chien Y, Kim S, Bumeister R, Loo YM, Kwon SW, Johnson CL, Balakireva MG, Romeo Y, Kopelovich L, Gale M Jr, et al. RalB GTPase-mediated activation of the IkappaB family kinase TBK1 couples innate immune signaling to tumor cell survival. Cell. 2006; 127:157–170. [PubMed: 17018283]

Chien Y, White MA. RAL GTPases are linchpin modulators of human tumour-cell proliferation and survival. EMBO Rep. 2003; 4:800–806. [PubMed: 12856001]

Clark K, Plater L, Peggie M, Cohen P. Use of the pharmacological inhibitor BX795 to study the regulation and physiological roles of TBK1 and IkappaB kinase epsilon: a distinct upstream kinase mediates Ser-172 phosphorylation and activation. J Biol Chem. 2009; 284:14136–14146. [PubMed: 19307177]

Dineen SP, Lynn KD, Holloway SE, Miller AF, Sullivan JP, Shames DS, Beck AW, Barnett CC, Fleming JB, Brekken RA. Vascular endothelial growth factor receptor 2 mediates macrophage infiltration into orthotopic pancreatic tumors in mice. Cancer Res. 2008; 68:4340–4346. [PubMed: 18519694]

Downward J. Targeting RAS signalling pathways in cancer therapy. Nat Rev Cancer. 2003; 3:11–22. [PubMed: 12509763]

Engelman JA. Targeting PI3K signalling in cancer: opportunities, challenges and limitations. Nature reviews. 2009; 9:550–562.

Fitzgerald KA, McWhirter SM, Faia KL, Rowe DC, Latz E, Golenbock DT, Coyle AJ, Liao SM, Maniatis T. IKKepsilon and TBK1 are essential components of the IRF3 signaling pathway. Nat Immunol. 2003; 4:491–496. [PubMed: 12692549]

Forbes SA, Tang G, Bindal N, Bamford S, Dawson E, Cole C, Kok CY, Jia M, Ewing R, Menzies A, et al. COSMIC (the Catalogue of Somatic Mutations in Cancer): a resource to investigate acquired mutations in human cancer. Nucleic Acids Res. 2009

Formstecher E, Aresta S, Collura V, Hamburger A, Meil A, Trehin A, Reverdy C, Betin V, Maire S, Brun C, et al. Protein interaction mapping: a Drosophila case study. Genome Res. 2005; 15:376–384. [PubMed: 15710747]

Fromont-Racine M, Rain JC, Legrain P. Toward a functional analysis of the yeast genome through exhaustive two-hybrid screens. Nat Genet. 1997; 16:277–282. [PubMed: 9207794]

Grindstaff KK, Yeaman C, Anandasabapathy N, Hsu SC, Rodriguez-Boulan E, Scheller RH, Nelson WJ. Sec6/8 complex is recruited to cell-cell contacts and specifies transport vesicle delivery to the basal-lateral membrane in epithelial cells. Cell. 1998; 93:731–740. [PubMed: 9630218]

Guertin DA, Stevens DM, Thoreen CC, Burds AA, Kalaany NY, Moffat J, Brown M, Fitzgerald KJ, Sabatini DM. Ablation in mice of the mTORC components raptor, rictor, or mLST8 reveals that mTORC2 is required for signaling to Akt-FOXO and PKCalpha, but not S6K1. Dev Cell. 2006; 11:859–871. [PubMed: 17141160]

Guo W, Sacher M, Barrowman J, Ferro-Novick S, Novick P. Protein complexes in transport vesicle targeting. Trends in cell biology. 2000; 10:251–255. [PubMed: 10802541]

Hacker H, Karin M. Regulation and function of IKK and IKK-related kinases. Sci STKE. 2006; 2006 re13.

Hiscott J. Convergence of the NF-kappaB and IRF pathways in the regulation of the innate antiviral response. Cytokine Growth Factor Rev. 2007; 18:483–490. [PubMed: 17706453]

Hresko RC, Mueckler M. mTOR.RICTOR is the Ser473 kinase for Akt/protein kinase B in 3T3-L1 adipocytes. The Journal of biological chemistry. 2005; 280:40406–40416. [PubMed: 16221682]

Ishikawa H, Barber GN. STING is an endoplasmic reticulum adaptor that facilitates innate immune signalling. Nature. 2008; 455:674–678. [PubMed: 18724357]

Ishikawa H, Ma Z, Barber GN. STING regulates intracellular DNA-mediated, type I interferon-dependent innate immunity. Nature. 2009; 461:788–792. [PubMed: 19776740]

Jacinto E, Facchinetti V, Liu D, Soto N, Wei S, Jung SY, Huang Q, Qin J, Su B. SIN1/MIP1 maintains rictor-mTOR complex integrity and regulates Akt phosphorylation and substrate specificity. Cell. 2006; 127:125–137. [PubMed: 16962653]

Kawai T, Akira S. Signaling to NF-kappaB by Toll-like receptors. Trends Mol Med. 2007; 13:460–469. [PubMed: 18029230]

Korherr C, Gille H, Schafer R, Koenig-Hoffmann K, Dixelius J, Egland KA, Pastan I, Brinkmann U. Identification of proangiogenic genes and pathways by high-throughput functional genomics: TBK1 and the IRF3 pathway. Proc Natl Acad Sci U S A. 2006; 103:4240–4245. [PubMed: 16537515]

Li X, Lu Y, Jin W, Liang K, Mills GB, Fan Z. Autophosphorylation of Akt at threonine 72 and serine 246. A potential mechanism of regulation of Akt kinase activity. J Biol Chem. 2006; 281:13837–13843. [PubMed: 16549426]

Manning BD, Cantley LC. AKT/PKB signaling: navigating downstream. Cell. 2007; 129:1261–1274. [PubMed: 17604717]

Mitin N, Rossman KL, Der CJ. Signaling interplay in Ras superfamily function. Curr Biol. 2005; 15:R563–R574. [PubMed: 16051167]

Moskalenko S, Henry DO, Rosse C, Mirey G, Camonis JH, White MA. The exocyst is a Ral effector complex. Nat Cell Biol. 2002; 4:66–72. [PubMed: 11740492]

Perry AK, Chow EK, Goodnough JB, Yeh WC, Cheng G. Differential requirement for TANK-binding kinase-1 in type I interferon responses to toll-like receptor activation and viral infection. J Exp Med. 2004; 199:1651–1658. [PubMed: 15210743]

Roland CL, Dineen SP, Lynn KD, Sullivan LA, Dellinger MT, Sadegh L, Sullivan JP, Shames DS, Brekken RA. Inhibition of vascular endothelial growth factor reduces angiogenesis and modulates immune cell infiltration of orthotopic breast cancer xenografts. Mol Cancer Ther. 2009; 8:1761–1771. [PubMed: 19567820]

Sarbassov, DD.; Guertin, DA.; Ali, SM.; Sabatini, DM. Science. Vol. 307. New York, N.Y: 2005. Phosphorylation and regulation of Akt/PKB by the rictor-mTOR complex; p. 1098-1101.

Sato S, Sugiyama M, Yamamoto M, Watanabe Y, Kawai T, Takeda K, Akira S. Toll/IL-1 receptor domain-containing adaptor inducing IFN-beta (TRIF) associates with TNF receptor-associated factor 6 and TANK-binding kinase 1, and activates two distinct transcription factors, NF-kappa B and IFN-regulatory factor-3, in the Toll-like receptor signaling. J Immunol. 2003; 171:4304–4310. [PubMed: 14530355]

Sharma S, tenOever BR, Grandvaux N, Zhou GP, Lin R, Hiscott J. Triggering the interferon antiviral response through an IKK-related pathway. Science. 2003; 300:1148–1151. [PubMed: 12702806]

Shiota C, Woo JT, Lindner J, Shelton KD, Magnuson MA. Multiallelic disruption of the rictor gene in mice reveals that mTOR complex 2 is essential for fetal growth and viability. Dev Cell. 2006; 11:583–589. [PubMed: 16962829]

Singh A, Greninger P, Rhodes D, Koopman L, Violette S, Bardeesy N, Settleman J. A gene expression signature associated with "K-Ras addiction" reveals regulators of EMT and tumor cell survival. Cancer cell. 2009; 15:489–500. [PubMed: 19477428]

Yamamoto M, Sato S, Hemmi H, Hoshino K, Kaisho T, Sanjo H, Takeuchi O, Sugiyama M, Okabe M, Takeda K, Akira S. Role of adaptor TRIF in the MyD88-independent toll-like receptor signaling pathway. Science. 2003; 301:640–643. [PubMed: 12855817]

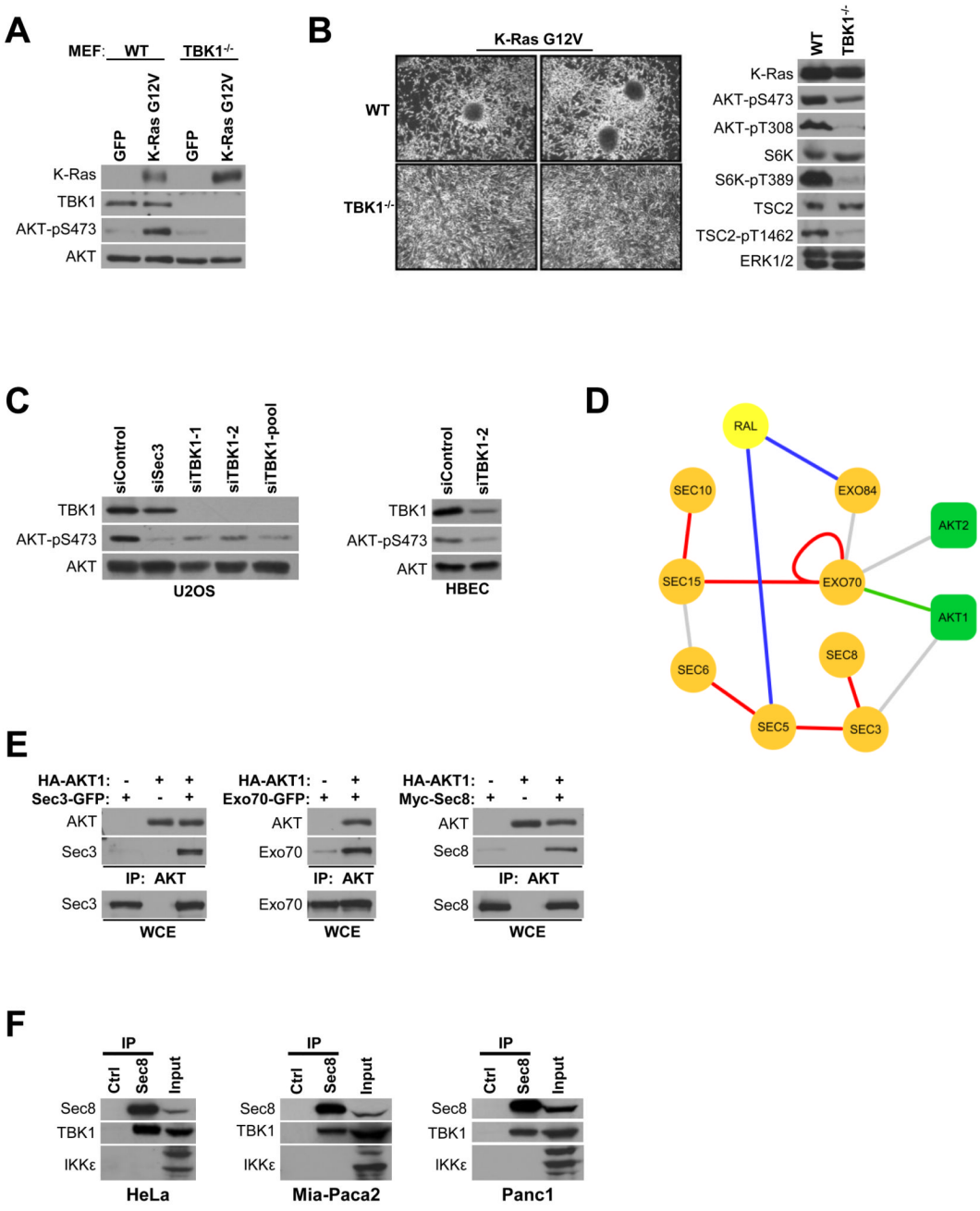

Figure 1. TBK1 and the exocyst support AKT activation

(A) Wild-type (WT) and TBK1 homozygous null (TBK1$^{-/-}$) mouse embryonic fibroblasts (MEF) were infected with lentivirus encoding GFP or K-RasG12V (Chien et al., 2006). Five days post-infection, whole cell lysates were prepared and relative accumulation of AKT-pS473, total K-Ras, TBK1, and AKT was assessed by immunoblot. (Approximate detected molecular size: K-Ras, 21KDa; TBK1, 84KDa; AKT, 60KDa; AKT-pS473, 60KDa; AKT-pT308, 60KDa)

(B) WT and TBK1$^{-/-}$ MEFs with equivalent stable expression of K-Ras G12V were seeded at low density and grown to confluence under standard culture conditions. Representative bright field images of monolayer cultures are shown (left panels). Whole cell lysates were

probed by immunoblot for the indicated proteins and selectively phosphorylated proteins (right panels). In addition to evaluation of AKT phosphorylation, the AKT substrate site on TSC2 (T1462) and the mTor-responsive site on p70S6K (T389) were evaluated as shown. ERK1/2 is shown as a loading control. (Approximate detected molecular size: AKT-pT308, 60KDa; S6K, 70KDa; S6K-pT389; TSC2, 200KDa; TSC2-pT1462, 200KDa; ERK1/2, 42/44KDa; others as described above)

(C) U2OS and HBEC cells were transfected with the indicated siRNAs. Seventy-two hours post transfection, whole cell lysates were assessed for TBK1 expression and accumulation of phosphorylated AKT as indicated. (Detected molecular sizes were as described above).

(D) The exocyst/Ral/AKT protein-protein interaction network as derived from whole-genome yeast two-hybrid screens. Edges are colored according to the confidence score attributed to each interaction in the screens (confidence score is detailed in (Formstecher et al., 2005)): red = A, blue = B, green = C, grey =D scores.

(E) HEK293T cells were transfected with the indicated constructs. 48 hours post transfection, AKT was immunoprecipitated using anti-HA beads and coprecipitating proteins were detected as indicated. Mammalian expression constructs encoding Sec3-GFP, Exo70-GFP, Myc-Sec8 and HA-AKT were transfected into HEK293T cells as indicated. IP indicates immunoprecipitation. WCE indicates whole cell extract. (Molecular size: Sec3, 102KDa; Exo70, 78KDa; Sec8, 110KDa; others as described above)

(F) Endogenous Sec8 was immunoprecipitated from the indicated cell lines using anti-Sec8 monoclonal antibodies. Immunoprecipitates were probed for endogenous TBK1 or IKKε as indicated. Anti-Myc monoclonal antibodies were used as a specificity control (Ctrl). (Molecular size: IKKε, a triplet centered on 80KDa; others as described above)

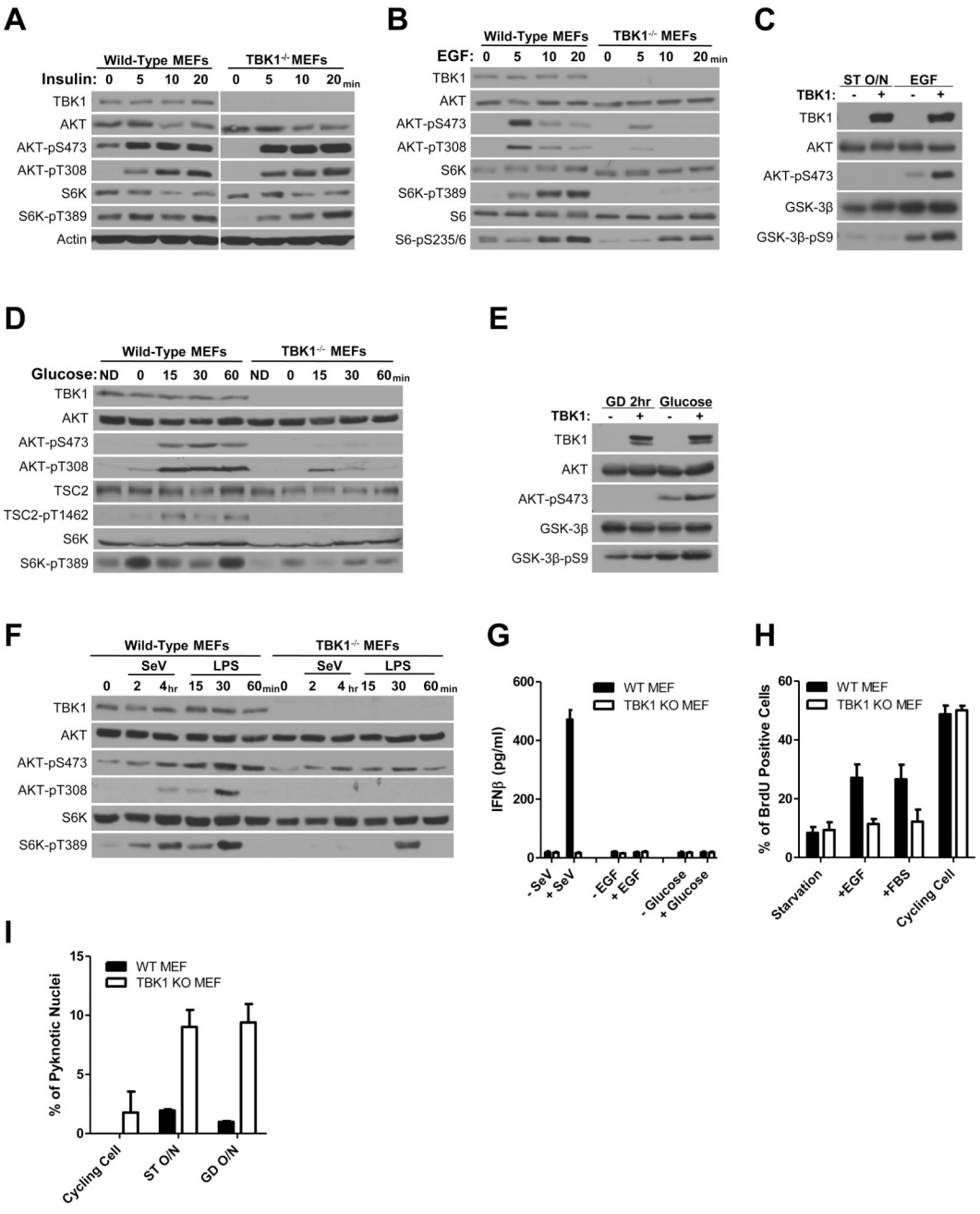

Figure 2. Selective contribution of TBK1 to stimulus-dependent AKT activation

(A) Wild-type and TBK1$^{-/-}$ MEFs were incubated overnight in the absence of serum and then treated with insulin (1 μg/ml) as indicated. Whole cell extracts were probed for the indicated proteins and selectively phosphorylated proteins. Actin is shown as a loading control. (Molecular size: Actin, 45KDa; others as described)

(B) Wild-type and TBK1$^{-/-}$ MEFs were incubated overnight in the absence of serum and then treated with EGF (100 ng/ml) as indicated. Whole cell extracts were probed as in (A). (Molecular size: S6, 32KDa; S6-pS235/6, 32KDa; others as described)

(C) TBK1$^{-/-}$ MEFs were infected with lentivirus encoding GFP or TBK1. Cell were starved without serum overnight (ST O/N) and then treated with EGF (100 ng/ml) as indicated.

Whole cell extracts were probed as in (A). The AKT substrate site on GSK3β (S9) was evaluated as an indication of AKT pathway activation. (Molecular size: GSK-3β, 46KDa; GSK-3β-pS9, 46KDa; others as described)

(D) Wild-type and TBK1$^{-/-}$ MEFs were incubated cells in DMEM with 10% serum but without glucose for 2 hours followed by addition of 25 mM glucose as indicated. Whole cell extracts were probed as in (A). ND indicates the normal DMEM control. (Molecular size: as described)

(E) TBK1$^{-/-}$ MEFs were infected with lentivirus encoding GFP or TBK1. Cells were incubated in DMEM with 10% serum but without glucose for 2 hours (GD 2hr) followed by addition of 25mM glucose as indicated. Whole cell extracts were probed as in (A). (Molecular size: as described)

(F) Wild-type and TBK1$^{-/-}$ MEFs were either exposed to Sendai virus (SeV, 100 HA/ml) or treated with LPS (1 μg/ml) as indicated. Whole cell extracts were probed as in (A). (Molecular size: as described)

(G) WT and TBK1$^{-/-}$ MEFs were either maintained in the presence of serum, serum starved, or glucose deprived overnight, and then treated with Sendai virus (SeV, 100 HA/ml), EGF (100 ng/ml), or glucose (25 mM) as indicated. After 19 hours, media was collected for measuring interferonβ accumulation. Error bars indicate standard error from the mean (SEM), N=3.

(H) WT and TBK1$^{-/-}$ MEFs were either maintained in the presence of serum (cycling cells) or serum starved 44 hr, and then treated with either EGF (100ng/ml) or FBS (10%) as indicated in the presence of BrdU (10 μM). BrdU incorporation is shown as a percentage of total nuclei. Error bars as in G.

(I) WT and TBK1$^{-/-}$ MEFs were either maintained in the presence of serum (cycling cells), serum starved, or glucose deprived. After 24hr cells were fixed and stained with DAPI. Pyknotic nuclei are shown as a percentage of total nuclei. Error bars as in G.

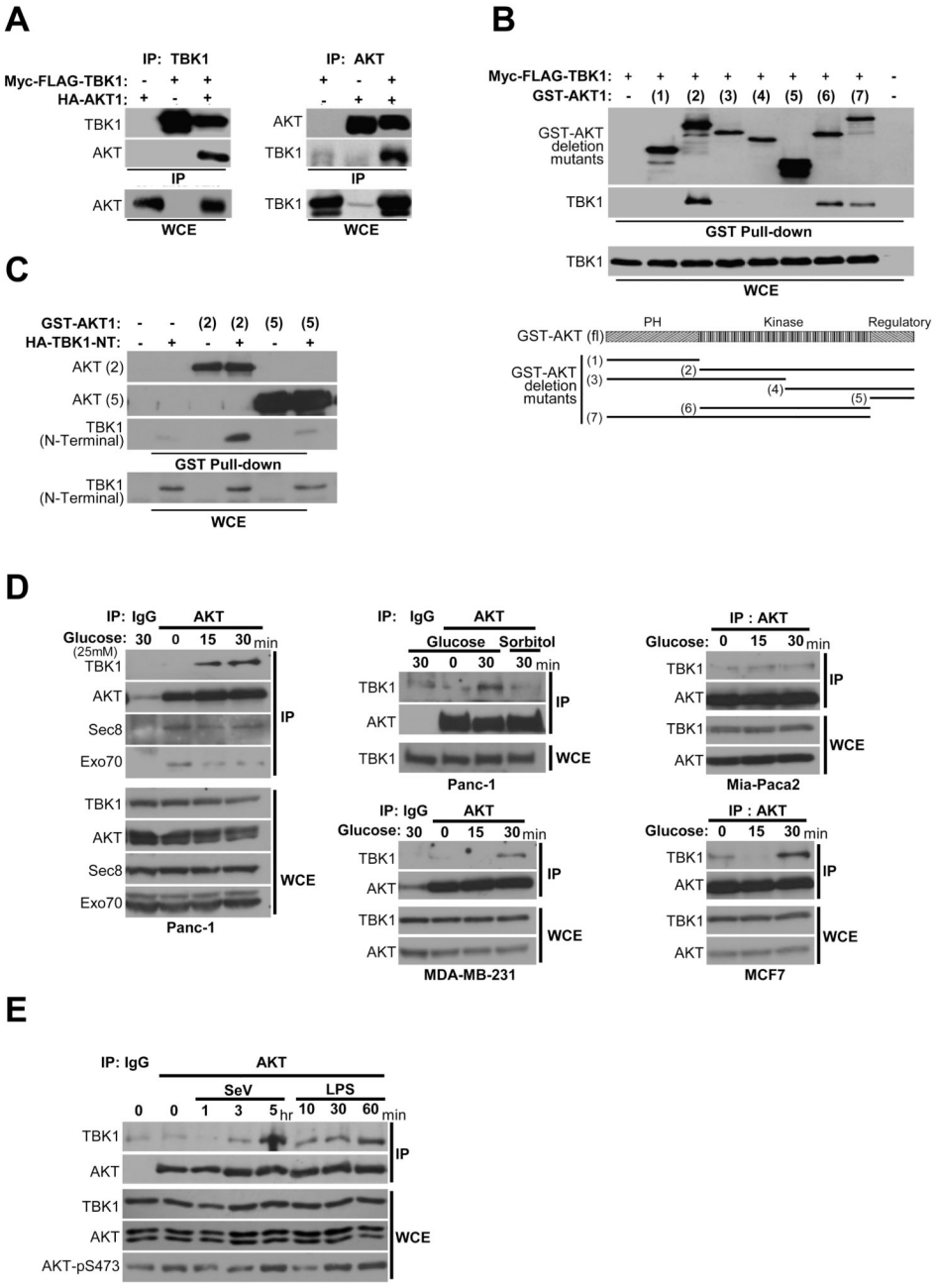

Figure 3. TBK1/AKT complex formation is stimulus-specific

(A) HEK293T cells were transfected as indicated. Reciprocal co-expression/co-immunoprecipitations are shown. (Molecular size: as previously described)

(B) GST-AKT expression constructs encoding a panel of truncation variants were coexpressed with Myc-FLAG-TBK1 in HEK293T cells. Glutathione-mediated affinity isolation of the AKT variants (GST Pull-down) was used to define a minimally sufficient TBK1 interaction domain as indicated. Whole cell extracts (WCE) are shown as controls for TBK1 expression.

(C) HA-tagged TBK1 amino-terminal fragment (1–242) that encompasses the catalytic domain [TBK1 (N-terminal)] was coexpressed with either GST-AKT expression constructs

[AKT(2)] or [AKT(5)]. Affinity isolation of AKT was probed for co-isolation of N-terminal TBK1as in (B).

(D) Panc-1, MDA-MB-231, Mia-Paca2, and MCF7 cells were deprived of glucose for 2 hr followed by incubation with 25 mM glucose or sorbitol as indicated. Endogenous AKT was immunoprecipitated from extracts taken at the indicated time points. Immunoprecipitates were assayed for coprecipitation of the indicated proteins. Normal mouse IgG was used as a control for specificity (IgG lanes). (Molecular size: as described)

(E) H1993 cells were either exposed to Sendai virus (SeV, 100 HA/ml) or treated with LPS (1 μg/ml), and harvested at the indicated time intervals. Co-immunoprecipitation and immunoblot were performed as in (D). Normal mouse IgG was used as a control for specificity (IgG lane). (Molecular size: as described)

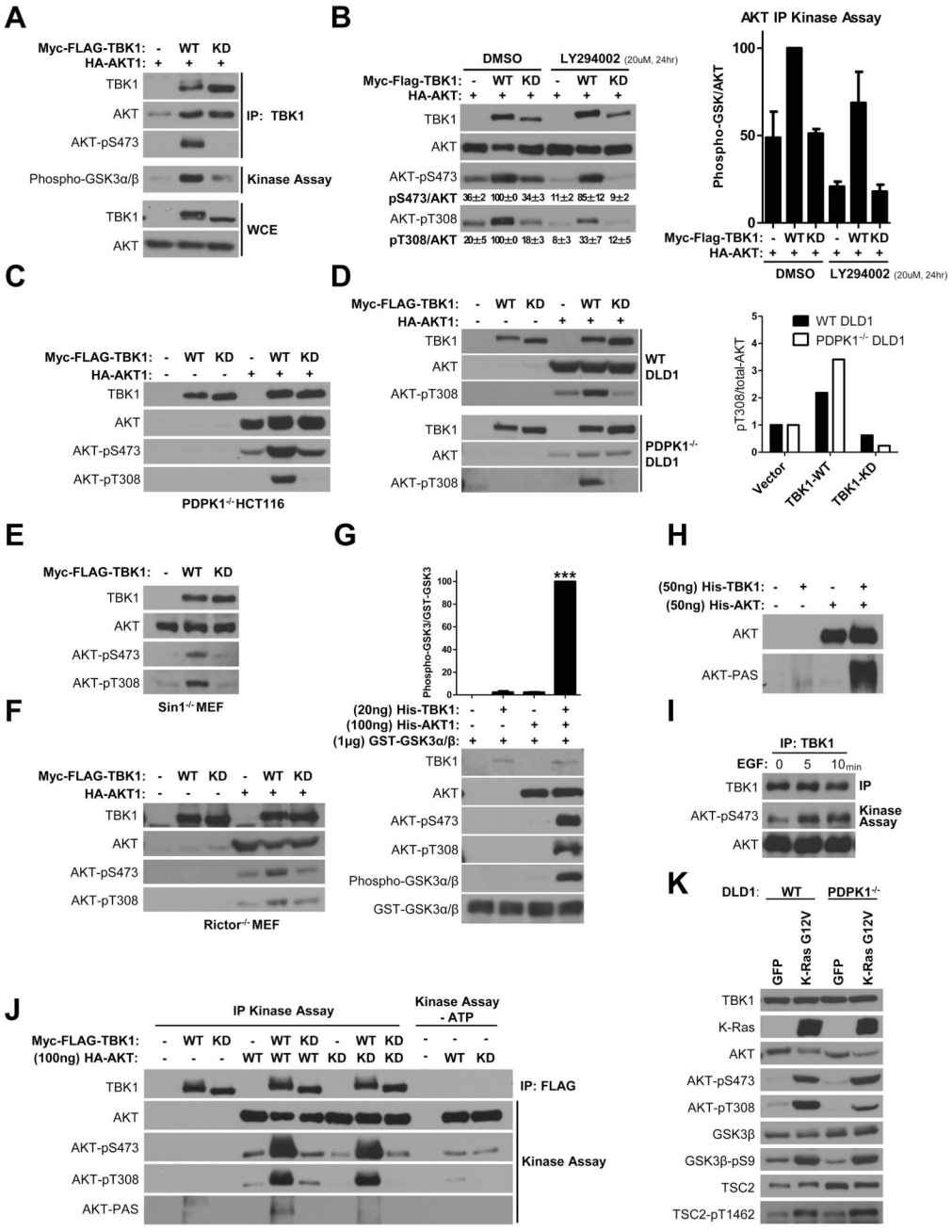

Figure 4. TBK1 directly activates AKT

(A) Myc-FLAG-tagged TBK1 was immunoprecipitated from HEK293T cells coexpressing HA-tagged AKT. Immunoprecipitates were probed for the presence of AKT and AKT-pS473 (IP). In addition, immunoprecipitates were assayed for AKT kinase activity, *in vitro*, using recombinant GST-GSK3α/β fusion peptides as substrate, and the phospho-GSK-3α/β (Ser21/9) antibody to detect substrate phosphorylation (Kinase Assay). Whole cell extracts (WCE) are shown as expression controls. (Molecular size: phospho-GST-GSK3α/β, 27KDa; others as described)

(B) HEK293T cells transfected as indicated were treated with DMSO or 20 μM LY294002 (PI3K inhibitor) for 24 hr prior to collection of protein extracts. Left panel: Whole cell

extracts probed with the indicated proteins are shown. AKT-pS473 and AKT-pT308 signal intensity was quantitated as a percent of total AKT. Values shown are the mean and standard errors from three experiments. Right panel: HA-tagged AKT was immunoprecipitated and AKT kinase activity in the immunoprecipitates was assayed as in (A) Error bars represent SDM from triplicate analyses (Right panel). (Molecular size: as described)

(C) PDPK1$^{-/-}$ HCT116 cells were transfected with plasmids encoding HA-AKT1, wild-type (WT) or kinase-dead (KD) TBK1 as indicated. Two days post-transfection, whole cell lysates were assessed for TBK1 and AKT expression, and accumulation of phosphorylated AKT as indicated. (Molecular size: as described)

(D) WT and PDPK1$^{-/-}$ DLD1 cells were transfected and treated as indicated in (C) (Left panel). Accumulation of AKT-pT308 signal intensity was normalized to total AKT signal intensity. Values are presented normalized to vector control (Right Panel). (Molecular size: as described)

(E) Sin1$^{-/-}$ MEFs were transfected with plasmids encoding wild-type (WT) or kinase-dead (KD) TBK1. Two day post-transfection, whole cell lysates were assessed for TBK1 expression and accumulation of phosphorylated AKT as indicated. (Molecular size: as described)

(F) Rictor$^{-/-}$ MEFs were transfected and treated as indicated in (C). (Molecular size: as described)

(G) Recombinant AKT and TBK1 proteins were incubated in kinase buffer with ATP at 30°C as indicated. After 30min incubation, GSK3α/β fusion peptides and additional ATP were added into each reaction at 30°C for an additional 30min. Reactions were separated by SDS-PAGE and immunoblotted to detect the indicated proteins and phosphorylation events. The products of kinase reactions were quantitated from multiple independent experiments. Error bars represent SEM from triplicate analysis. Significance was evaluated by One-way ANOVA, Bonferroni's Multiple Comparison Test. ***, indicates $p<0.0001$.

(H) The indicated purified recombinant proteins were incubated in kinase buffer with ATP at 30°C for 30min. Reactivity of recombinant AKT (top panel) with anti-phospho-AKT substrate site (R-X-R-X-X-pS/pT) antibodies (PAS) is shown (bottom panel).

(I) WT MEFs were serum starved overnight and then treated with EGF (100 ng/ml) as indicated. Endogenous TBK1 was immunoprecipitated and assayed for TBK1 kinase activity, *in vitro*, using recombinant His-AKT protein as substrate, and the anti-pS473-AKT antibody to detect substrate phosphorylation (Kinase Assay).

(J) Immunopurified Myc-FLAG-tagged TBK1 wild-type (WT) or kinase-dead (KD) was incubated with purified inactive HA-tagged AKT wild-type (WT) or kinase-dead (KD) as indicated. Kinase reactions were separated by SDS-PAGE and immunoblotted to detect the indicated proteins and phosphorylation events. (Molecular size: AKT-PAS: 70KDa; others as described)

(K) WT and PDPK1$^{-/-}$ DLD1 were infected with lentivirus encoding GFP or K-RasG12V. Three days post-infection, whole cell lysates were prepared and probed by immunoblot for the indicated proteins and selectively phosphorylated proteins. (Molecular size: as described)

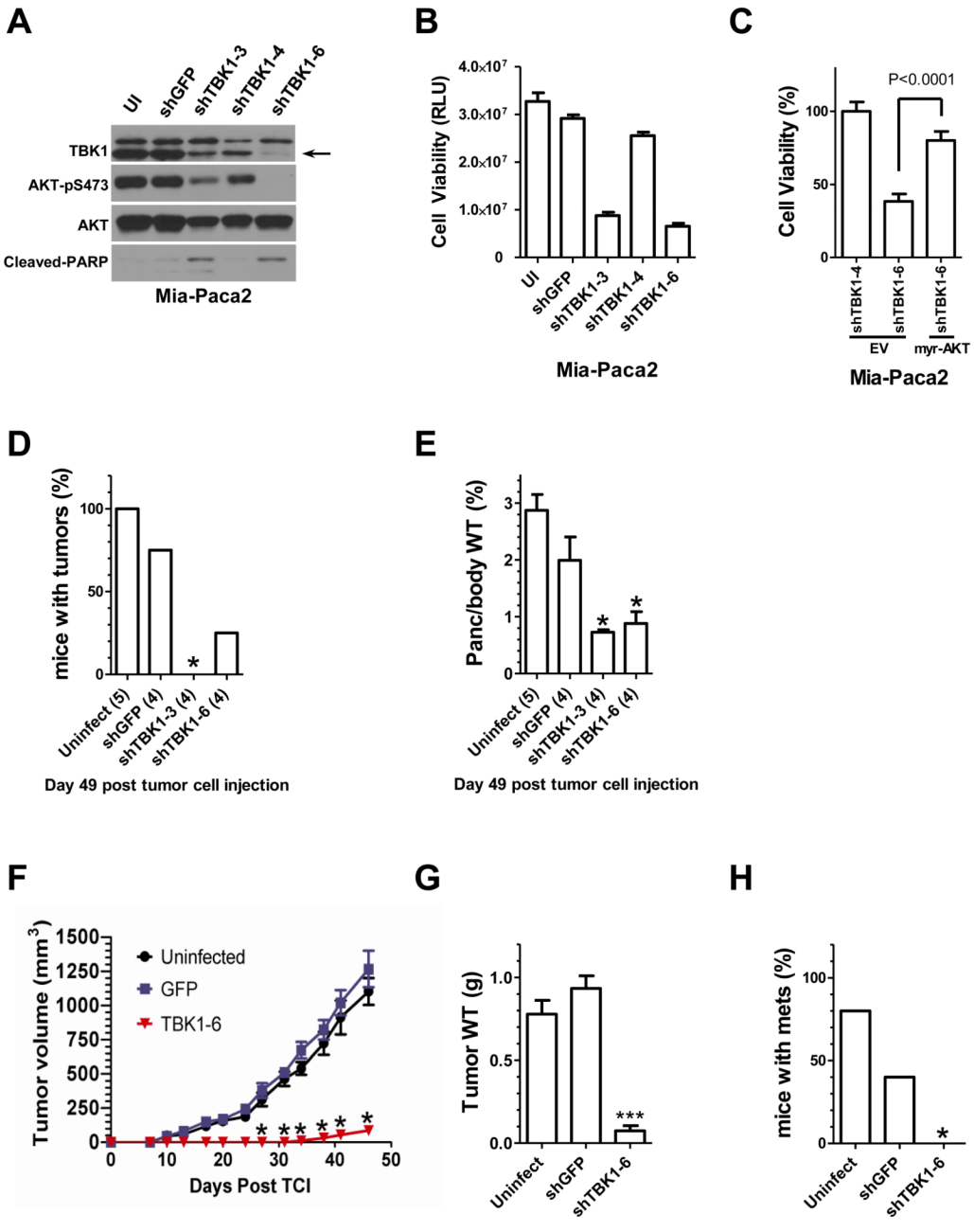

Figure 5. TBK1 is required to support cancer cell tumorigenicity *in vivo*

(A) Mia-Paca2 cells were infected with lentivirus encoding shRNAs targeting GFP (shGFP) or TBK1 (shTBK1–3, shTBK1–4 and shTBK1–6). UI indicates uninfected control. Three days post-infection, whole cell extracts were assayed for the indicated proteins. (Molecular size: as previously described)

(B) Mia-Paca2 cells were treated as in (A), and assayed for relative viability 6 days post-infection using an ATP-coupled luminescence assay (CellTiter-Glo, Promega). Bars indicated standard deviation from the mean of three independent experiments.

(C) Mia-Paca2 cells were transfected with plasmids encoding a constitutively active variant of AKT (myr-AKT) or empty vector (EV) as a control (Bellacosa et al., 1998). One-day

post-transfection, cells were infected as indicated in (A) with lentivirus encoding shTBK1–4 and shTBK1–6. Five-day post-infection, cell viability was assayed as in (B). Bars indicate SDM from triplicate experiments. Significance was evaluated using the student's two-tailed T-test.

(D) 1×10^6 Mia-Paca2 cells uninfected (n=5) or stably expressing GFP (n=4) or shRNA constructs targeting TBK1 (TBK1–3, n=4; TBK1–6; n=4) were injected into the pancreas of SCID mice. All cells were collected two days post lentiviral infection and viability was confirmed by trypan blue exclusion. At this time-point, TBK1 depletion has not proceeded to the point that begins to engage cell death. Animal health and tumor growth was monitored and a cohort of animals sacrificed on Day 49 post tumor cell injection. Total tumor incidence is shown. N is indicated in parentheses.

(E) Pancreas weight (tumor burden) was normalized to total body weight at the end of the study and is displayed as % of body weight. Bars indicate SDM. N is indicated in parentheses.

(F) MDA-MB-231 cells uninfected or stably expressing GFP or shRNA targeting TBK1 (TBK1–6) (n=5/group, bars indicate SDM) were injected into the mammary fat pad of female SCID mice. Again, all cells were collected two days post lentiviral infection and viability was confirmed by trypan blue exclusion. Animal health and tumor volume were followed throughout the duration of the experiment.

(G) Tumor burden at the time of sacrifice is displayed as final tumor weight. Bars indicate SDM, N=5/group.

(H) Metastatic incidence. N=5/group.

(D–H) *, indicates $p<0.05$; and ***, indicates $p<0.005$ vs. uninfected control by ANOVA with a Bonferroni correction for multiple comparison testing.

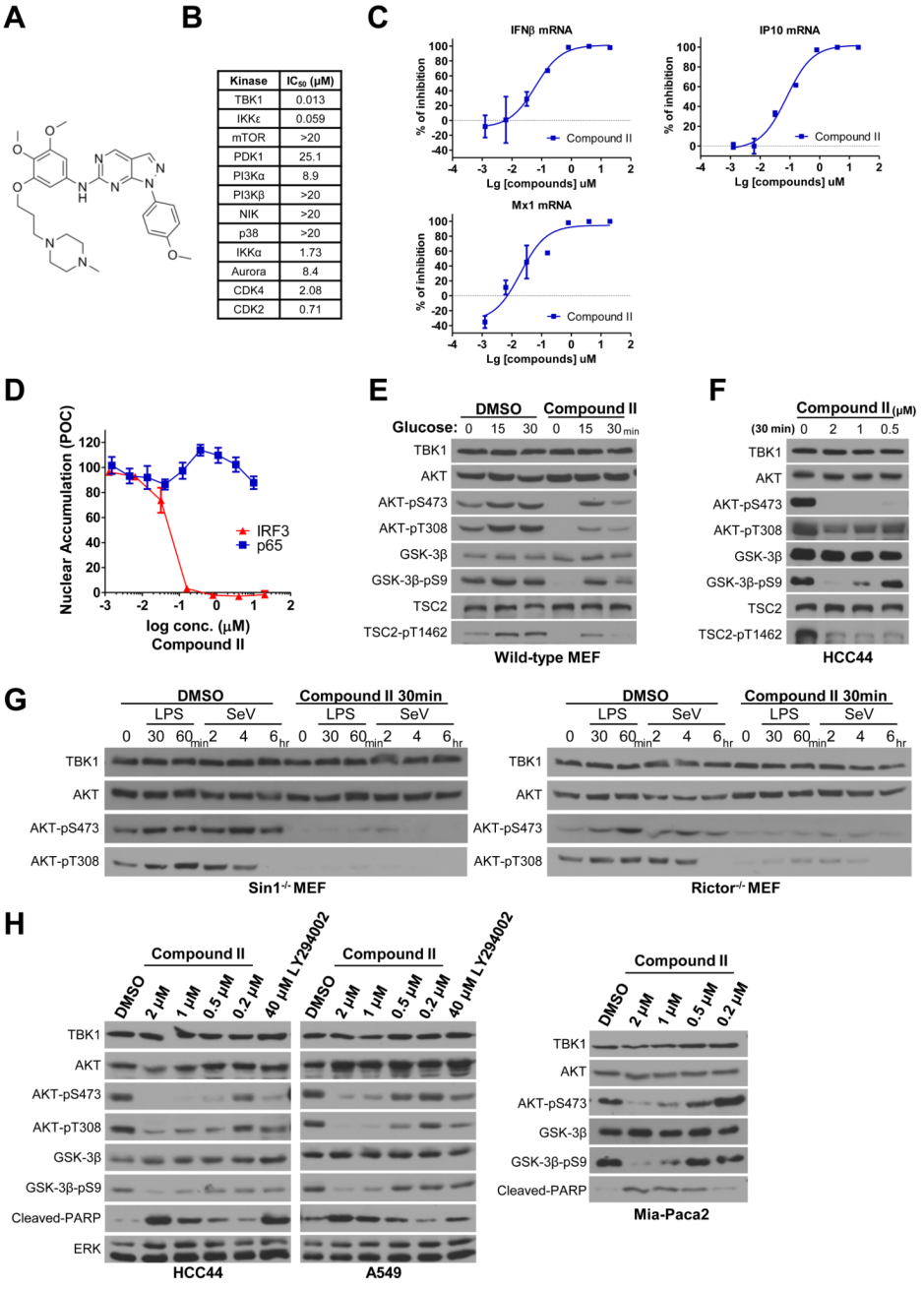

Figure 6. Pharmacological inhibition of TBK1 impairs AKT signaling

(A) Structure of Compound II.

(B) IC_{50} values for *in vitro* inhibition of the indicated purified recombinant kinases by Compound II.

(C) Primary macrophages from mouse bone marrow were treated with LPS and increasing concentrations concentration of Compound II. LPS induced accumulation of interferonβ (IFNβ) and interferonβ target gene (IP10 and Mx1) mRNAs were measured by quantitative PCR and shown as percent of inhibition. Error bars represent SDM from triplicate experiments.

(D) HeLa cells incubated in the indicated concentrations of Compound II were stimulated with 10 ng/ml TNFα for 10 minutes (p65 assays), or transfected with poly I:C for 2 hours (IRF3 assays), followed by immunofluorescence-based detection of IRF3 and p65 nuclear accumulation. Nuclear accumulation is plotted as percent of control (POC). Error bars represent SDM from triplicate analysis.
(E) Wild-type MEFs were incubated cells in DMEM with 10% serum but without glucose for 2 hours. Cells were then pretreated with 2 μM Compound II for 30 minutes as indicated followed by addition of 25 mM glucose as indicated. Whole cell extracts were prepared post glucose stimulation and immunoblotted as shown. (Molecular size: as described)
(F) Asynchronous proliferating cultures of HCC44 cells were exposed to the indicated concentrations of Compound II for 30 minutes. Whole cell extracts were immunoblotted for detection of the indicated proteins and phospho-proteins. (Molecular size: as described)
(G) $Sin1^{-/-}$ and $Rictor^{-/-}$ MEFs were pretreated with DMSO or Compound II for 30 minutes as indicated, followed by exposure to LPS (1 μg/ml) or Sendai virus (SeV, 100 HA/ml). Whole cell extracts prepared at the indicated time-points were immunoblotted for detection of AKT activation. (Molecular size: as described)
(H) Whole cell extracts from HCC44, A549 and Mia-Paca2 cells exposed to the indicated concentrations of Compound II or LY294002 for 24 hours were immunoblotted to detect consequences on AKT pathway activation. (Molecular size: cleaved-PARP: 89KDa; others as described)

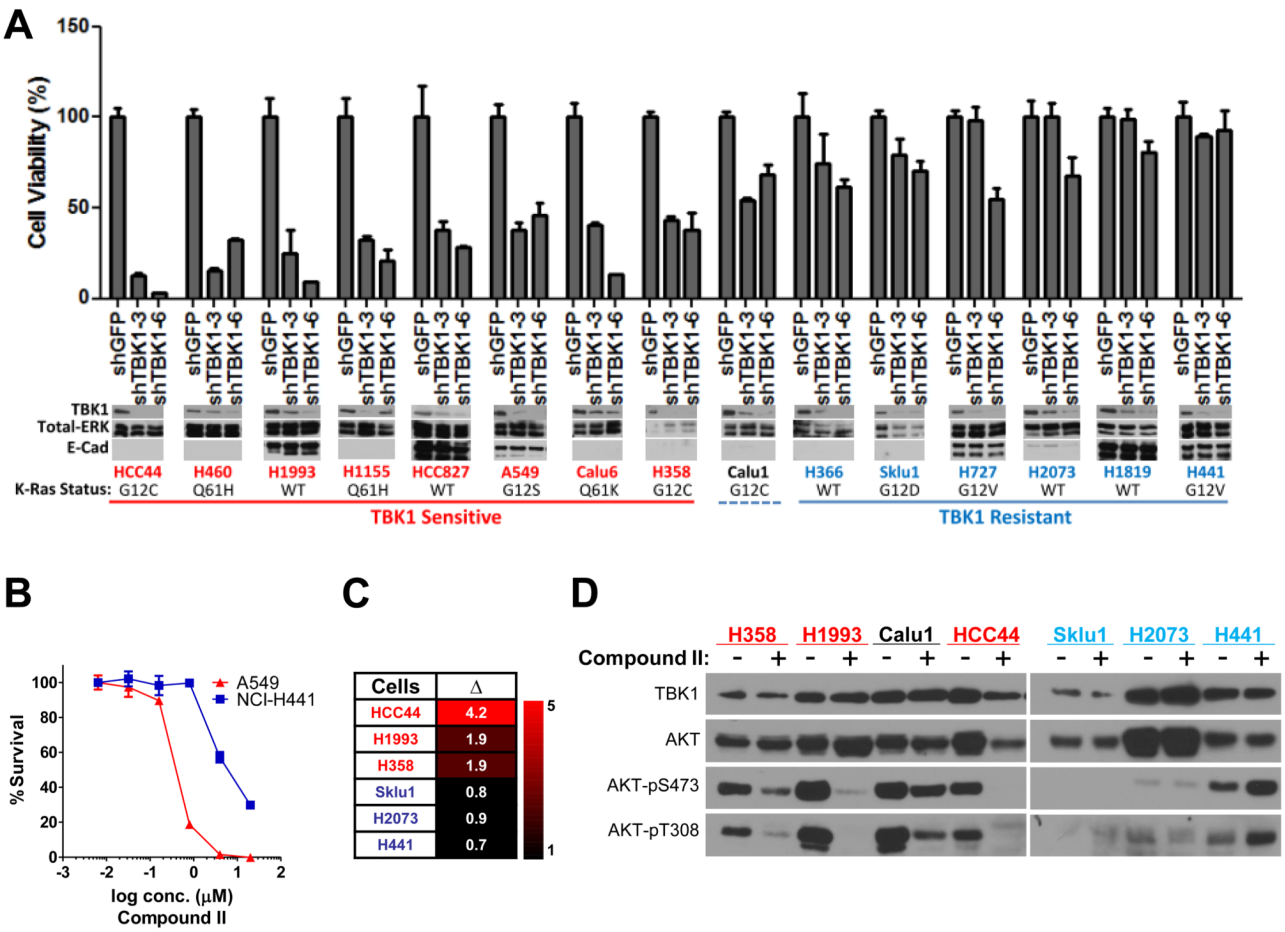

Figure 7. TBK1 sensitivity in non small cell lung cancer

(A) The indicated cell lines were infected with lentivirus encoding shRNAs targeting GFP or two independent shRNAs targeting TBK1 as indicated. Relative cell viability was assayed 6 days post infection as in Figure 5. Error bars indicate SDM from triplicate experiments. Whole cell extracts from parallel infections were collected and probed for the indicated proteins. (Molecular size: E-Cadherin, 135KDa; others as previously described)

(B) Following a 96-hour exposure to the indicated concentrations of Compound II, A549 and H441 cell viability was measured as indicated. Bars represent SDM from triplicate experiments.

(C) The indicated cell lines were exposed to DMSO or 2 μM Compound II for 24 hours. Cells were then labeled with FITC-conjugated Annexin V, and scored by FACS. Values shown in the heatmap represent fold-induction of Annexin V positive cells over the DMSO controls (Δ).

(D) Whole cell extracts from cells treated for 24 hours as in (C) were immunoblotted as indicated. Lysates were loaded based on equivalent cell numbers for each sample. (Molecular size: as previously described)